

# INDIAN IEEY GEOMAGNETIC OBSERVATIONAL PROGRAM AND SOME PRELIMINARY RESULTS

B.R. Arora, M.V. Mahashabde and R. Kalra

Indian Institute of Geomagnetism  
Colaba, Bombay 400 005, India

As part of an India coordinated program for the IEEY, five fluxgate magnetometer stations, ideally placed to investigate the fine latitudinal structure of the equatorial electrojet (EEJ), counter electrojet (CEJ) and their return currents, have been added to the already existing Indian chain of permanent geomagnetic observatories, extending from the dip equator up to the latitude of the Sq-focus. The disposition of temporary IEEY stations was facilitated by the ground magnetic survey undertaken to identify the true course of the meandering dip equator. Observations are being made in regular as well as in intensive campaign mode in close coordination with ionospheric observations in India and elsewhere on the globe. The first intensive observation campaign was undertaken during January 7-30, 1992. The quiet-day variations from this campaign are used to provide provisional estimate of electrojet parameters which significantly differ from that reported using POGO satellite data. The nature of daily variation in Declination (D) suggests active interplay between northern and southern Sq vortices in the form of successive intrusion and withdrawal of the southern hemispheric current system up to the 10°N dip latitude. The spatial structure of the vertical field (Z) variations indicates dominance of induction effects. Greater understanding of the contribution of sub-surface conductivity anomalies to internal currents is desired before the Z data can be used as constraints in deducing the parameters of electrojet currents. The data from the enhanced network suggest that the latitudinal width of the CEJ currents does not exceed the width of the electrojet. The mapping of the fine structure of the CEJ related perturbation at equatorial as well as low- and mid-latitudes provides a good case to simulate observations numerically to identify the most effective tidal wind modes in producing CEJ events.

**O PROGRAMA OBSERVACIONAL GEOMAGNÉTICO DA ÍNDIA PARA O AIEE E ALGUNS RESULTADOS PRELIMINARES** *Cinco novas estações com magnetômetros tipo fluxgate foram acrescentadas à rede de instrumentos geomagnéticos da Índia entre o equador geomagnético e a latitude de foco do sistema  $S_q$ . A escolha dos locais foi cuidadosamente planejada para permitir a investigação da estrutura fina do eletrojato equatorial (EJE), do eletrojato reverso (EJR) e suas correntes de retorno. A distribuição destas estações de monitoramento temporário para o AIEE foi facilitada pelo trabalho anterior de levantamento magnético de superfície para determinar a posição do equador. As observações estão sendo realizadas em condições normais e em campanhas intensivas coordenadas com observações ionosféricas na Índia e em outros locais. A primeira campanha intensiva de observações foi realizada de 7 a 30 de janeiro de 1992. As variações de dias calmos desta campanha são usadas para estimativas preliminares de parâmetros do eletrojato que diferem substancialmente daqueles obtidos usando dados do satélite POGO. O padrão de variações diurnas em declinação (D) sugere uma interação ativa entre os vórtices de norte e do sul, na forma de sucessivas entradas e saídas do sistema de correntes do hemisfério sul até a latitude dip de 10° N. A estrutura espacial das variações do campo vertical (Z) indica o domínio do efeito de indução. É desejável que se tenha uma melhor compreensão da contribuição de anomalias nas condutividades debaixo da superfície sobre correntes internas, antes de se poder usar os dados de Z como parâmetros para deduzir os elementos das correntes do eletrojato. Os dados da rede aumentada sugerem que a extensão latitudinal das correntes do EJR não excedem aquela do EJ. O mapeamento da estrutura fina da perturbação relacionada ao EJR em latitudes equatoriais, baixas e médias, fornece um bom caso para simular observações numericamente e assim identificar os modos de marés dos ventos que seriam mais eficientes para produzir eventos do EJR.*

## INTRODUCTION

With the discovery of the phenomenon of equatorial electrojet (EEJ), magnetic field variations have been extensively used to study the latitudinal structure and temporal variability of the electrojet with respect to local time, longitude, day-to-day, season and solar cycle. (For review see Onwumechili, 1967; Forbes, 1981; Reddy, 1989). Despite the continuous research since its first discovery (Bartels and Johnston, 1940; Chapman, 1951), some of the fundamental questions, e.g. whether the EEJ is an independent current system with its own return flow or if it forms a part of the planetary Sq current system, still remain unresolved. Investigations aimed to resolve these issues often need to decompose the observed variation into electrojet ( $S_R^E$ ) and planetary ( $S_R^P$ ) components. Forbes (1981) noting that separation of observed fields into  $S_R^E$  and  $S_R^P$  requires data over a much greater latitude range than has been considered in many previous studies, suggested that some contradictory inferences on the relationship of the EEJ with world-wide Sq current system may stem from this inadequate separation.

The choice of the physical model selected to define the electrojet currents realistically is constrained by the number of magnetic observatories recording field variations both under and away from the electrojet. When data from only a few stations are available, this is achieved either by adopting a very simple model for the electrojet or by employing data of the vertical field component. The vertical field variations due to their vulnerability to the internal induced currents are less reliable for the purpose of estimating electrojet parameters. Further, a better understanding of the spatial and temporal characteristics of counter electrojet (CEJ) related variations, as compared to normal days, would greatly facilitate to apply the hierarchy of numerical simulation scheme and identify the causative mechanism of the CEJ within the framework of tidal theory. Recognizing that to

understand the full vagaries of the EEJ and the CEJ, a dense network of geomagnetic observatories is a basic pre-requisite, the permanent network of magnetic observatories from near the dip equator to the region of Sq-focus in India has been augmented by adding five more temporary stations with fluxgate magnetometers. The locations of the permanent magnetic observatories functional during the IEEY are shown in Fig. 1 which includes a newly commissioned observatory at Nagpur (NAG). The locations of the new temporary stations set up in peninsular India as a part of all India co-ordinated program for IEEY are shown in Fig. 2. The geographic and geomagnetic co-ordinates together with the dip latitude for all observatories are given in Table 1. Giving a brief account of factors controlling the disposition of new stations, the observational strategy to coordinate measurements with aeronomic experiments is discussed before proceeding to present the preliminary results emerging from the analysis of initial data set obtained from the first intensive observational campaign.

## DIP EQUATOR AND LAYOUT OF MAGNETOMETER CHAIN

It is now well established that the dip equator has a meandering path. The central axis of the electrojet is expected to be inalienably linked with the dip equator. To optimally plan the stations's disposition in relation to the dip equator, a ground based geomagnetic survey was carried out, as a prelude to the IEEY activity, to locate the exact path of the dip equator across India (Rangarajan and Deka, 1991). In this survey, spot measurements of the ambient vertical field ( $Z$ ) component were made every 4-5 km along three north-south profiles traversing along the west coast, east coast and the spine of peninsular India (Fig. 3). The line of zero- $Z$  in the contour plot (Fig. 3) marks the location of the dip equator for the year 1991, which is found to follow a curved path. Fig. 3 also shows the location of the dip equator for 1971 and 1981, delineated by earlier field surveys

**Table 1.** Geographic and geomagnetic co-ordinates of geomagnetic observatories functional during the IEEY along the Indian sector.

*Coordenadas geográficas e geomagnéticas dos observatórios geomagnéticos em funcionamento durante o AIEE no setor Indiano.*

Observatory	Code	Geographic		Geomagnetic		Dip Lat	Co-ordinator
		Lat Deg	Long Deg	Lat Deg	Long Deg		
Gulmarg	GUL	34.05	74.40	24.90	148.84	32.11	IIG
Sabhawala	SAB	30.37	77.80	20.93	151.50	27.35	SOI
Ujjain	UJJ	23.18	75.78	13.97	148.83	18.42	IIG
Nagpur	NAG	21.15	79.08	11.64	151.74	15.74	IIG
Alibag	ABG	18.63	72.86	9.74	145.55	12.96	IIG
Hyderabad	HYD	17.42	78.55	7.97	150.87	11.16	NGRI
Anantapur	ANT	14.67	77.63	5.32	149.71	7.83	IEEY
Bangalore	BAN	12.98	77.60	3.64	149.52	5.75	IEEY
Annamalainagar	ANN	11.37	79.68	1.85	151.39	3.67	IIG
Karur	KAR	11.01	78.09	1.64	149.80	3.32	IEEY
Kodaikanal	KOD	10.23	77.46	0.92	149.11	2.37	IIA
Virudunagar	VIR	9.61	77.94	0.26	149.52	1.61	IEEY
Ettiapuram	ETT	9.17	78.02	-0.19	149.56	1.06	NGRI
Trivandrum	TRD	8.48	76.95	-0.77	148.44	0.28	IIG
Kanyakumari	KAN	8.10	77.54	-1.21	148.98	-0.23	IEEY

Co-ordinating Institutions:

IIG - Indian Institute of Geomagnetism

IIA - Indian Institute of Astrophysics

NGRI - National Geophysical Research Institute

SOI - Survey of India

IEEY - Network set up by IIG

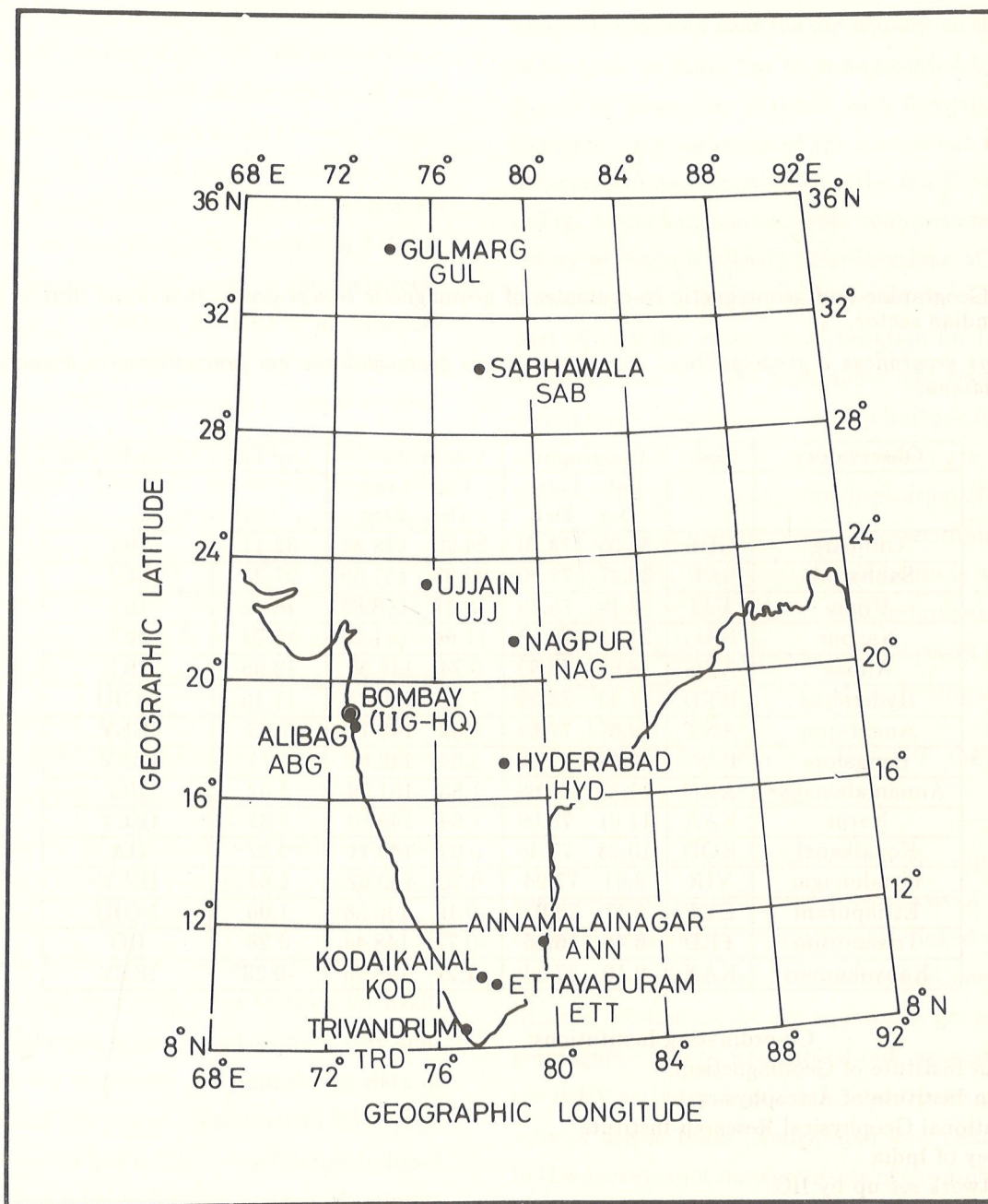


**Figure 1.** Distribution of Indian geomagnetic observatories from near the dip equator to the region of Sq-focus. Nagpur is a new observatory established in late 1991.

*Distribuição dos observatórios geomagnéticos Indianos entre o equador dip e a região de foco Sq. Nagpur é um observatório novo estabelecido no final de 1991.*

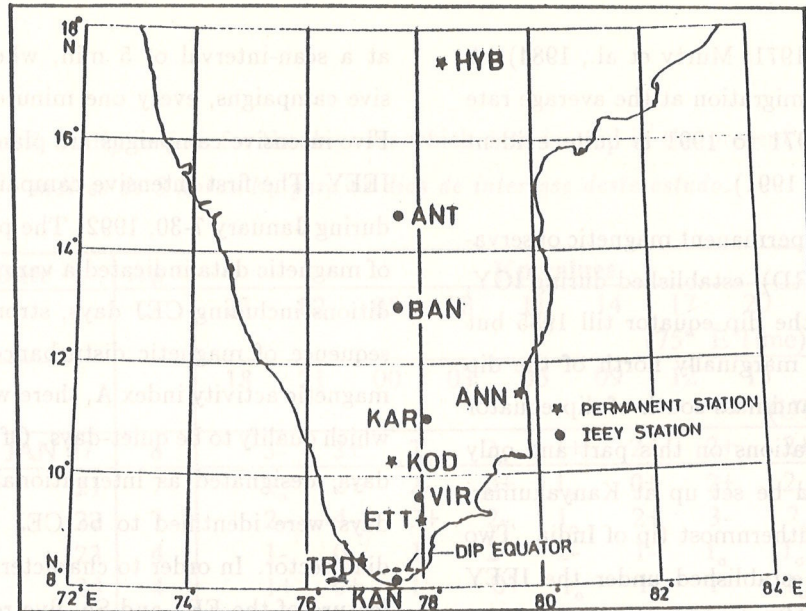


**Figure 2.** Locations of five temporary fluxgate magnetometers, set up as part of the IEEY campaign, filling vital gaps in the existing network of observatories in Peninsular India. The upgraded network is in operation since October, 1991.

*Localização de cinco magnetômetros fluxgate temporários, instalados como parte da campanha do AIEE, preenchendo importantes vazios na rede de observatórios existentes na Índia peninsular. A rede otimizada está em operação desde outubro de 1991.*

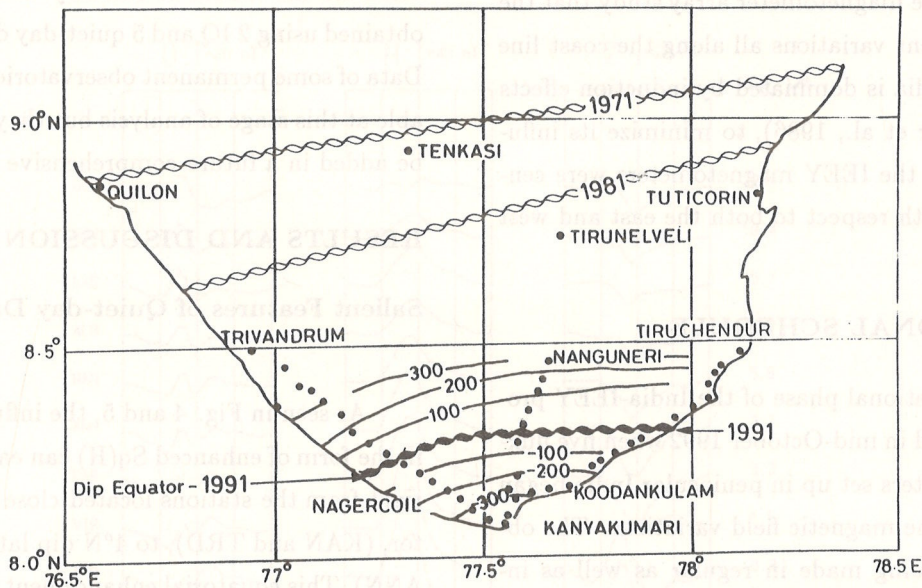


**Figure 3.** Contour plot of ambient vertical field component ( $Z$ ) at the southern tip of India, based on the measurement at sites (solid circles) occupied during geomagnetic survey undertaken during February, 1991 to delineate ground position of the dip equator. Deduced location of dip equator for 1991, corresponding to the contour of zero- $Z$ , is shown in relation to its position in 1971 and 1981, inferred based on similar survey undertaken earlier (Based on Rangarajan and Deka, 1991).

*Curvas de contorno do componente de campo vertical ( $Z$ ) ambiente no extremo sul da Índia, obtidas de medidas especiais obtidas nos locais indicados (círculos) durante o levantamento geomagnético de fevereiro de 1991, para obter a localização na superfície do equador dip. A localização do equador dip para 1991, correspondendo ao contorno de  $Z$  zero, está mostrada em relação à sua posição em 1971 e 1981, deduzida através de levantamentos semelhantes anteriores (ver Rangarajan e Deka, 1991).*

(IIG, NGRI, and SOI, 1971; Murty et al., 1984). A well defined southward migration at the average rate of 4 km/yr between 1971 to 1991 is quite evident (Rangarajan and Deka, 1991).

The southernmost permanent magnetic observatory at Trivandrum (TRD), established during IGY, was situated south of the dip equator till 1985 but at present it is placed marginally north of the dip equator. The limited landmass south of dip equator restricted number of stations on this part and only one IEEY station could be set up at Kanyakumari (KAN), right at the southernmost tip of India. Two of the magnetometers established under the IEEY chain, viz. BAN and ANT, in addition to filling the large gap between the permanent observatories ANN and HYB, were positioned to facilitate mapping of return currents of the EEJ, expected to peak around  $\pm 5\text{-}6^\circ$  dip latitude (Onwumechili, 1992). Given the evidence from the magnetometer array study that the nature of transient variations all along the coast line of peninsular India is dominated by induction effects (e.g. see Thakur et al., 1986), to minimize its influence the sites of the IEEY magnetometers were centrally located with respect to both the east and west coast lines.

## OBSERVATIONAL SCHEDULE

The observational phase of the India-IEEY program commenced in mid-October 1992 when five flux-gate magnetometers set up in peninsular India began registration of the magnetic field variations. The observations are being made in regular as well as intensive campaign mode. During intensive campaigns, magnetic observations are supplemented by measurements using a variety of sensors including ionosonde, VHF back scatter and HF radars, optical interferometers etc, to permit an integrated interpretation of physical processes controlling the EEJ. (Arora and Somayajulu, 1991). During regular mode, the magnetic registration of three components is carried out

at a scan-interval of 5 min, whereas during intensive campaigns, every one minute value is recorded. Five intensive campaigns are planned over the entire IEEY. The first intensive campaign was undertaken during January 7-30, 1992. The preliminary scrutiny of magnetic data indicated a variety of magnetic conditions including CEJ days, strong EEJ and a long sequence of magnetic disturbances. Judged by the magnetic activity index A, there were a very few days which qualify to be quiet-days. Of the five most quiet-days, designated as international quiet days, three days were identified to be CEJ days along the Indian sector. In order to characterize the conspicuous feature of the EEJ and Sq, five relatively quiet days were selected from the month of February 1992. The  $A_P$  index and eight 3-hr  $K_P$  indices corresponding to local days selected for analysis are given in Table 2. Fig. 4 and Fig. 5 give the average quiet-day Sq variation for the month of January and February 1992, obtained using 2 IQ and 5 quiet-day data respectively. Data of some permanent observatories were not available at this stage of analysis but they are expected to be added in a future comprehensive study.

## RESULTS AND DISCUSSION

### Salient Features of Quiet-day Daily Variations

As seen in Fig. 4 and 5, the influence of the EEJ in the form of enhanced Sq(H) can easily be identified right from the stations located close to the dip equator, (KAN and TRD), to  $4^\circ\text{N}$  dip latitude (KAR and ANN). This equatorial enhancement of Sq(H) against the background global Sq variation is more clearly marked on Fig. 6(a), which shows the plot of quiet-day range, reckoned as the difference in the principal diurnal maximum and minimum, as a function of dip latitude. Following a sharp drop in magnitude near the edge of the electrojet ( $4^\circ$  dip latitude), the regular Sq(H) with a near-noon maximum decreases in magnitude with increasing latitude, vanishing almost at

**Table 2.** Daily  $A_p$  and 3-Hr  $K_p$  indices for the days for which data is used in the present study.

*Valores diários de  $A_p$  e índices de 3 horas  $K_p$  para os dias de interesse deste estudo.*

Date	$A_p$	Kp values									
		23	02	05	08	11	14	17	20	23	
		(75° E Time)									
		18	21	00	03	06	09	12	15	18	
		(UT Hr)									
1992 JAN 07	8	3-	3+	2 <sub>o</sub>	2 <sub>o</sub>	1+	2+	2+	2+	2+	
21	7	2 <sub>o</sub>	2+	2-	0+	1 <sub>o</sub>	0+	2+	2 <sub>o</sub>	2 <sub>o</sub>	
22	7	2-	4-	3+	2-	1 <sub>o</sub>	2+	3-	2 <sub>o</sub>	2 <sub>o</sub>	
23	4	1-	0 <sub>o</sub>	1-	2-	2-	1-	1 <sub>o</sub>	1 <sub>o</sub>	1 <sub>o</sub>	
24	4	1+	0+	1 <sub>o</sub>	0+	1 <sub>o</sub>	1 <sub>o</sub>	1-	1 <sub>o</sub>	1 <sub>o</sub>	
24	4	1-	2 <sub>o</sub>	3-	2 <sub>o</sub>	1-	1 <sub>o</sub>	1+	0+	0+	
1992 FEB 05	7	5 <sub>o</sub>	5-	3 <sub>o</sub>	1 <sub>o</sub>	2-	2+	2+	1+	1+	
06	7	1-	1 <sub>o</sub>	1 <sub>o</sub>	1+	2-	2-	3 <sub>o</sub>	2 <sub>o</sub>	2 <sub>o</sub>	
11	7	3 <sub>o</sub>	2+	2+	1+	2-	2-	2-	2+	2+	
15	4	2+	3-	0+	2-	1+	1 <sub>o</sub>	2 <sub>o</sub>	1 <sub>o</sub>	1 <sub>o</sub>	
16	4	0+	1-	1 <sub>o</sub>	1+	1+	0+	1+	1 <sub>o</sub>	1 <sub>o</sub>	

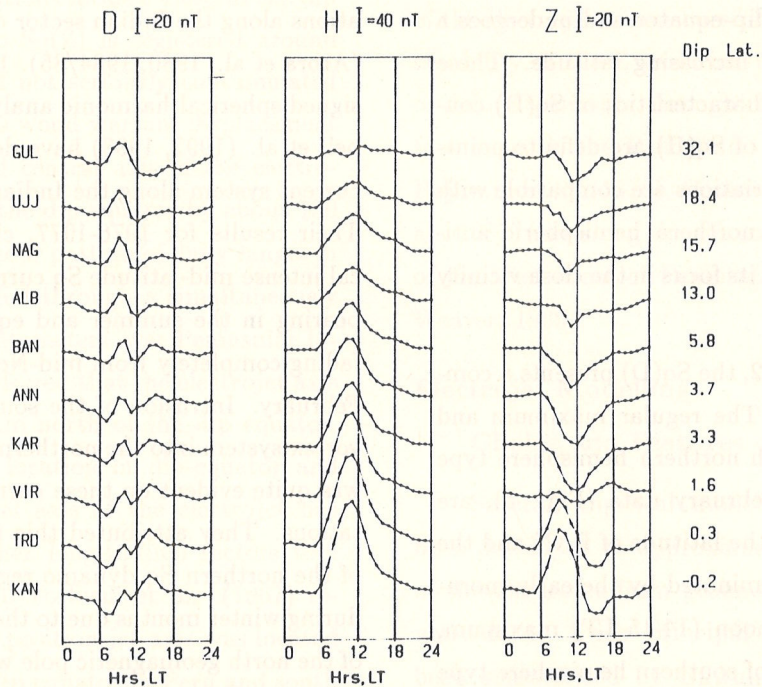


**Figure 4.** Average quiet-day variations,  $S_q$ , in D, H and Z obtained using data of January, 1992 from a network of permanent and temporary stations functional during the first intensive observational campaign of the IEEY.

*Variações médias de dia calmo,  $S_q$ , nas componentes D, H, e Z obtidas usando dados de janeiro de 1992 de uma rede de estações permanentes e temporárias em operação durante a primeira campanha intensiva de observação para o AIEE.*

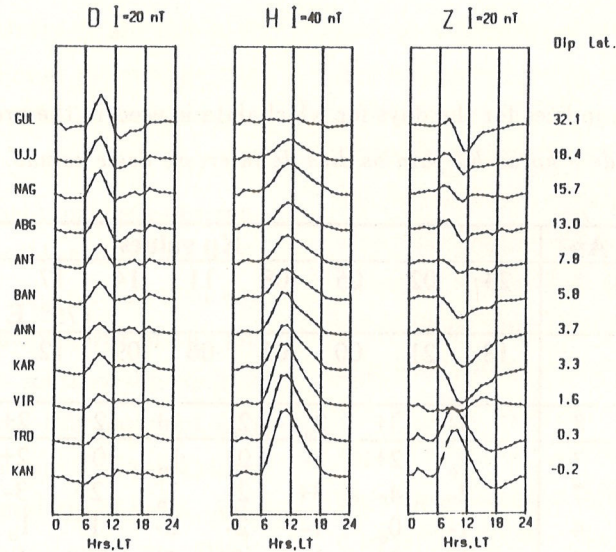


**Figure 5.** Same as Fig. 4 but for the data of February, 1992.

*O mesmo que na Fig. 4, mas com dados para fevereiro, 1992.*

GUL. During February, 1992 (Fig. 5), the  $Sq(D)$  is characterized by easterly maximum around 8-10 LT and minimum around 13-14 LT. The magnitude of  $Sq(D)$  is small near the dip-equator and undergoes a systematic increase with increasing latitude. These diurnal and latitudinal characteristics of  $Sq(D)$  coupled with the signatures of  $Sq(H)$  are definite pointers that observed  $Sq$  - variations are compatible with that expected from the northern hemispheric anti-clockwise  $Sq$  vortex, with its focus in the close vicinity of the latitude of GUL.

During January 1992, the  $Sq(D)$  presents a complex pattern (Fig. 4). The regular maximum and minimum associated with northern hemisphere type  $Sq(D)$ , as seen in the February data (Fig. 5), are highly attenuated up to the latitude of BAN and the diurnal variations are dominated by the early morning minimum and afternoon (14-15 LT) maximum, which are characteristic of southern hemisphere type  $Sq(D)$  variations. The presence of signatures related to both northern and southern hemisphere  $Sq$  current vortices suggests that during January 1992, the daily variations at selected hours of the day are controlled by variable intrusion of southern hemispheric

currents into the northern hemisphere up to even  $18^{\circ}N$ . Such intrusions of the southern current to the north were shown to be regular features of daily variations along the Indian sector during winter solstices (Arora et al., 1980, 1984/85). Using the specially designed spherical harmonic analysis technique, Campbell et al. (1992, 1993) have derived the ionospheric current system along the Indian Central Asia sector. Their results for 1976-1977, clearly showed a typical intense mid-latitude  $Sq$  current system vortex appearing in the summer and equinoctial months but fading completely from mid-November through mid-February. Intrusion of the southern hemispheric  $Sq$  vortex system into the northern hemisphere in winter was quite evident on these current contour representations. They attributed this to the lower exposure of the northern  $Sq$  dynamo region to solar radiation during winter months due to the off-spin axis position of the north geomagnetic pole with respect to the line of observatories along the Indian sector (Campbell et al., 1993).



### Dominant Induction Effects

In the equatorial belt the latitudinal characteristics of  $Sq(Z)$  are sensitive to the spatial gradients in the electrojet source currents. Locations characterized by zero- $Sq(Z)$  and maximum  $Sq(Z)$  respectively demarcate the ground projection of the central axis and edge of the electrojet and define the half-width of the electrojet (Chapman, 1951). Apart from the effects of the spatial structure of source currents, the  $Z$ -variations are also prone to internal induced current system, largely determined by the sub-surface electrical conductivity distribution which is now known to be highly anomalous all along the coastal belt of the Indian Peninsula (Rajaram et al., 1976; Thakur et al., 1986; Srivastava 1992 and references therein). The significantly large  $Sq(Z)$  at KAR and ANN could be consistent with the edge effect of the electrojet but the abnormally large  $Sq(Z)$  at TRD and KAN are certainly anomalous for stations located close to the dip equator. The near-zero  $Sq(Z)$  is registered around VIR (+ 1.6° dip lat). If not seriously contaminated by induction effects, this would warrant displacement of the ground projected central axis of the electrojet towards north from the dip equator by about 150 km. Examining the contour pattern of daily ranges in  $Sq(Z)$  and  $Sq(H)$  recorded through a simultaneously operated array of magnetometers over Peninsular India, Srivastava (1992) inferred that the electrojet axis was located about 55 km north of the dip equator. Such mismatch in the location of dip-equator and ground projected central axis of the electrojet has been reported from other longitudinal sectors too. Davis et al. (1967) and Forbush et al. (1967) reported that the ground position jet axis was located 20-50 km north of the dip equator in Peru and south of the dip equator in Nigeria. Cain (1969), demonstrating that the dip equator shifts from its ground position by about 33 km per 100 km altitude in the South American zone, ascribed the observed difference in the dip equator and ground projected cen-

tral axis to the latitudinal shift of the dip equator at the height of electrojet source currents. Based on the IGRF model for 1990, along the Indian sector, the offset between the location of the dip equator at ground and at a height of 107 km - the seat of the electrojet currents in India (Sampath and Sastry, 1979) - is only about 5 km, smaller by more than one order of the deduced shift. Furthermore, if the location of the observed near-zero  $Sq(Z)$  variation marked the true ground electrojet axis, such profound displacement with respect to the dip equator should also be reflected as a northward shift in the peak in the latitudinal profile of  $Sq(H)$  ranges. In contrast to this, the observed latitudinal profile (Fig. 6(a)) of ranges in  $Sq(H)$ , shows a clear maximum located between TRD and KAN, almost coinciding with the present location of the dip equator. The difference in the disposition of near zero- $Z$  and maximum  $H$  variation, rather than reflecting the complex spatial structure of the electrojet source current may manifest the vulnerability of the  $Z$  variation to complex channelling of induced currents through the deep seated conductors beneath the Palk Strait (Thakur et al., 1986; Rajaram et al., 1976), Comorin Ridge (Mareschal et al., 1987) and along the rift zone aligned with the tip of the west coast of Peninsular India (Agarwal and Weaver, 1989).

### Electrojet Modelling

#### Choice and Features of Model

Several empirical modeling formulations have been developed to approximate physical parameters of the electrojet from ground or rocket-based magnetic data. Their principal features have recently been summarized by Onwumechili (1992). In the present work, continuous distribution of current density model of Onwumechili (1965a, b, 1967) has been used. The model has the advantage that, in its generalized form, it allows for both latitudinal and vertical variation of current intensity. It can also easily be

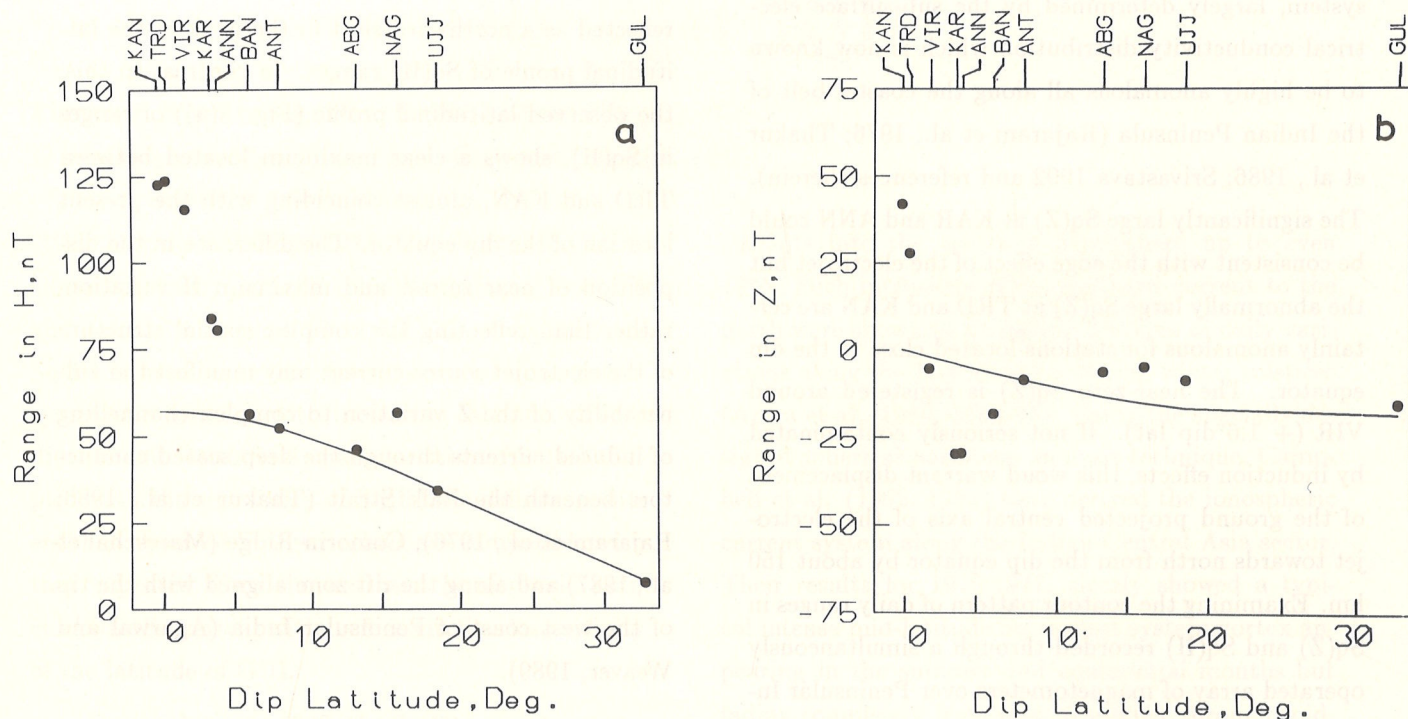


**Figure 6.** Plot showing latitudinal dependence of quiet-day (Sq) ranges in (a) H and (b) Z. Solid curve marks the extrapolation of global-Sq part into the equatorial region. Departures of observed ranges at equatorial stations are reckoned as measure of part associated with the electrojet.

*Variação latitudinal do sistema Sq para (a) H e (b) Z. A curva sólida marca a extrapolação da parte global de Sq para a região equatorial. Desvios das variações observadas em estações equatoriais são aceitas como uma medida de parte associada com o eletrojato.*

reduced to a form suitable for the study of latitudinal distributions of the eastward height integrated current intensity when only ground based data are available for the determination of electrojet parameters. In this modified form the eastward current intensity ( $J$ , A/km) at a distance  $x$  from the central axis of electrojet current is given by:

$$J = J_0 \frac{a^2(a^2 + \alpha x^2)}{(a^2 + x^2)} \quad (1)$$

where  $J_0$  is peak current intensity at the central axis, ( $x = 0$ ),  $a$  is constant scale length related to half width ( $\omega = a\sqrt{-\alpha}$ ) and  $\alpha$  is a dimensionless constant controlling the meridional distribution of electrojet currents,  $\alpha \geq 0$  symbolizes unidirectional (eastward) current but  $\alpha < 0$  implies presence of westward (return) current on the flanks of the magnetic dip equator. The evidence on the existence of the return currents and its physical implications have critically been reviewed by Onwumechili (1992).

The full expressions for the magnetic fields associated with current function in eq.(1) and the analysis procedure to determine  $a$ ,  $\alpha$  and  $J_0$  from observational data are detailed in Onwumechili (1967) and, hence, are not repeated here. Only certain simplifications and approximations made in its adoption to Indian data are mentioned briefly to evaluate their impact on final results.

### Estimation of Sq under electrojet

In the initial step towards separating observed fields, i.e. daily ranges in Sq(H) and Sq(Z), into the world-wide Sq and electrojet parts, the latitudinal behavior of global-Sq field is expressed by a function similar to eq. (1). The  $a$ ,  $\alpha$  and  $J_0$  defining Sq-model parameters were determined using observed ranges of Sq(H) from three widely separated stations, namely GUL, UJJ, and ANT, all located away from the influence of the electrojet. Fig. 6(a) gives the estimated variations of global Sq(H) ranges as a function of latitude using parameters  $a$ ,  $\alpha$  and  $J_0$  derived from the

data of February 1992. The computed Sq(H) curve (Fig. 6(a)) provides a good fit to all low-latitude stations except at NAG. The anomalous character of the variation at NAG needs to be investigated when a much more complete data base becomes available from this newly commissioned observatory.

Given the sensitivity of Z variations to induction effects, following Onwumechili (1967), the extrapolation of Sq(Z) into the electrojet belt is not obtained by fitting eq. (1) to observed Sq(Z) ranges but rather adopting  $a$ ,  $\alpha$ , and  $K$  ( $= 0.2\pi J_0$ ) obtained using Sq(H) data. Prior to their adoption, intensity parameter  $K$  is reduced by a factor, equivalent to the ratio of internal to external parts of Sq, to account for the sign of internal field contribution to total observed Sq(Z) variations. Incorporating this factor for the Indian sub-continent to be 0.38 (Campbell et al. 1993), the estimated latitudinal profile of computed Sq(Z) is shown in Fig. 6(b). The poor fit between computed and observed Z ranges may merely arise from the heterogeneous character of the electrical conductivity distribution at depth. However, it is worthy of note that extrapolated Sq(Z) profile, in agreement with the expected behavior, attains a zero-value near the dip equator, in close proximity with the axis of maximum Sq(H). Furthermore, within the equatorial belt, with the exception of KAN and TRD the departures of observed ranges with respect to the estimated Sq-profile, both in H and Z show a spatial pattern compatible with the electrojet currents and can, thus, be reckoned as a measure of the electrojet field.

### Decomposition of electrojet fields into external and internal parts

The isolated electrojet fields in H and Z, plotted as a function of dip latitude, were interpolated onto a regular spacing using quasi-Hermite splines which have the property of being continuous with a continuous first derivative. The interpolated regularly

spaced data were then Hilbert transformed (KH, KZ) by Fourier transformation to separate the observed electrojet field in H and Z into external ( $H_e$ ,  $Z_e$ ) and internal ( $H_i$ ,  $Z_i$ ) parts using the relations:

$$H_e = 1/2(H + KZ); H_i = 1/2(H - KZ)$$

$$Z_e = 1/2(Z - KH); Z_i = 1/2(Z + KH)$$

In the absence of data from the south of the dip equator, for purpose of Hilbert transformation of the latitude profile, the smooth H curve obtained by fitting quasi-Hermite splines to the electrojet field values upto 6°N dip latitude, were mirrored symmetrically with respect to the peak value into the opposite hemisphere. In case of Z, the values were mirrored anti-symmetrically to account for the reversal in the sign of Z-fields at the dip equator. The Z values at KAN and TRD were ignored as they are dominated by induction effects and the Z-field was assumed to be zero at the latitude where the H electrojet field attained maximum.

#### Determination of the electrojet parameters

Finally the estimated external jet field in H were used to obtain fit to eq. (1) to approximate major parameters of the electrojet ( $a$ ,  $\alpha$  and  $K (=0.2\pi J_0)$ ). These fittings, using data of February 1992, yielded  $a = 6.7^\circ$ ;  $\alpha = -2.20$ ;  $K = 72.0$  nT. Substituting these values in the relation  $K = 0.2\pi J_0$  and  $\omega = a/\sqrt{-\alpha}$ , we get peak intensity and half-width ( $\omega$ ) of the electrojet current for Feb. 1992 to be of the order of 114.6 A/km and 4.1° (450 km).

Table 2 summarizes the parameters of the Indian electrojet derived by several workers. A persistently lower value of halfwidth in all earlier results compared to the present value of about 450 km, may be because of the basic differences in models. All earlier workers used uniform hand model of constant intensity through the entire width of current and is, therefore, bound to yield lower value than in the model

where current intensity decreases to zero at the edge of the electrojet. The variability of each parameter in the earlier results largely depict the seasonal/solar activity dependence.

The most comprehensive attempt to model electrojet parameters is that of Onwumechili and Agu (1981(a), (b)) and Ozoemena and Onwumechili (1987), using POGO satellite data. Their results are nearest for comparison with the present one because of identical model, though data employed come from epochs of markedly different solar activity. Comparison of the present value of  $\omega$  and  $J_0$  with landmark values for the global average or that corresponding to the longitudinal sector of 45-90°E (given in Table 3a and b) show the estimate of  $\omega$  for Feb. 92 is about twice the global average, whereas peak current intensity ( $J_0$ ) is only half of the value for POGO data.

The negative sign of the meridional distribution parameter  $\alpha$  is consistent with earlier results based on ground, satellite and rocket data, but its present estimate of -2.20 is little lower than the most commonly reported value of -1.83 based on POGO or rocket data (Onwumechili, et al., 1989a; Onwumechili, 1992). Incorporating these values in the expressions:

$$J_m = J_0[\alpha^2/4(\alpha - 1)]$$

and

$$x_m^2 = a^2(\alpha - 2)/\alpha$$

suggests that the peak intensity of westward return current ( $J_m$ ) is placed at a distance ( $x_m$ ) of about 930 km and has magnitude of -46 A/km. The higher value of peak intensity ( $J_0$ ) for POGO data compared to the present value may simply be the result of differences in the level of solar activity but it is hard to ascertain whether the present higher values of half-width ( $\omega$ ) and distance of peak westward return current ( $x_m$ ) in relation to POGO values mark the inverse relation between intensity and half-width reported by

**Table 3a.** Half-width ( $w$ ) and Peak intensity ( $J_o$ ) of the electrojet currents along Indian sector and global averages (Based on Uniform Band Model).

*Largura ( $w$ ) e intensidade máxima ( $J_o$ ) das correntes de eletrojato do setor Indiano e médias globais (Modelo de banda uniforme).*

Region	Mode of Magnetic Data	Period	Half-width ( $w$ ) in km	Peak intensity ( $J_o$ ) Amp/km	
India	Ground	April-Aug 1958-59	300	87	Yacob and Khanna (1963)
India	Ground	April-Aug 1958	$297 \pm 2$	$100 \pm 4$	Yacob (1967)
India	Ground	April-Aug 1964	$275 \pm 1$	$59 \pm 3$	- do -
India	Ground	Annual 1976	$146 \pm 46$	$93 \pm 24$	Srivastava (1992)
India	Ground	Annual 1980	$169 \pm 39$	$128 \pm 43$	- do -

**Table 3b.** Half-width ( $w$ ) and Peak intensity ( $J_o$ ) of the electrojet currents along Indian sector and global averages (Based on Continuous Distribution of Current Intensity Model).

*Largura ( $w$ ) e intensidade máxima ( $J_o$ ) das correntes de eletrojato do setor Indiano e médias globais (Modelo de distribuição contínua de Intensidade de corrente).*

Region	Mode of Magnetic Data	Period	Half-width ( $w$ ) in km	Peak intensity ( $J_o$ ) Amp/km	
Global	POGO Satellite	Equinoxial 1967-69	$235 \pm 14$	$232 \pm 63$	Onwumechili and Agu (1981a)
Indian Sector	POGO Satellite	Equinoxial 1967-69	227	241	- do -
Global	POGO Satellite	Solstices 1967-69	$226 \pm 11$	$207 \pm 28$	Ozoemena and Onwumechili (1987)
Indian Sector	POGO Satellite	Solstices 1967-69	228	189	- do -
India	Ground	February 1992	450	115	Present Study

Onwumechili and Agu (1981b) and Onwumechili et al. (1989b) or provide further corroboration to the results of Onwumechili and Ozoemena (1985) that  $\omega$  and  $x_m$  estimated from ground-based data generally tend to be greater than the distances derived from satellite data.

Onwumechili et al. (1989a) ascribed this disagreement to some basic differences arising from the processing of the ground and satellite data. Two possible factors indicated by them relate to the underestimation of worldwide Sq in the ground data or the overestimation of electrojet signature in the satellite profile (Onwumechili et al., 1989a). However, the different sensitivity of ground and satellite magnetic data to local induction effects may also contribute to the mismatch.

## SEQUENCE OF COUNTER ELECTROJET EVENTS

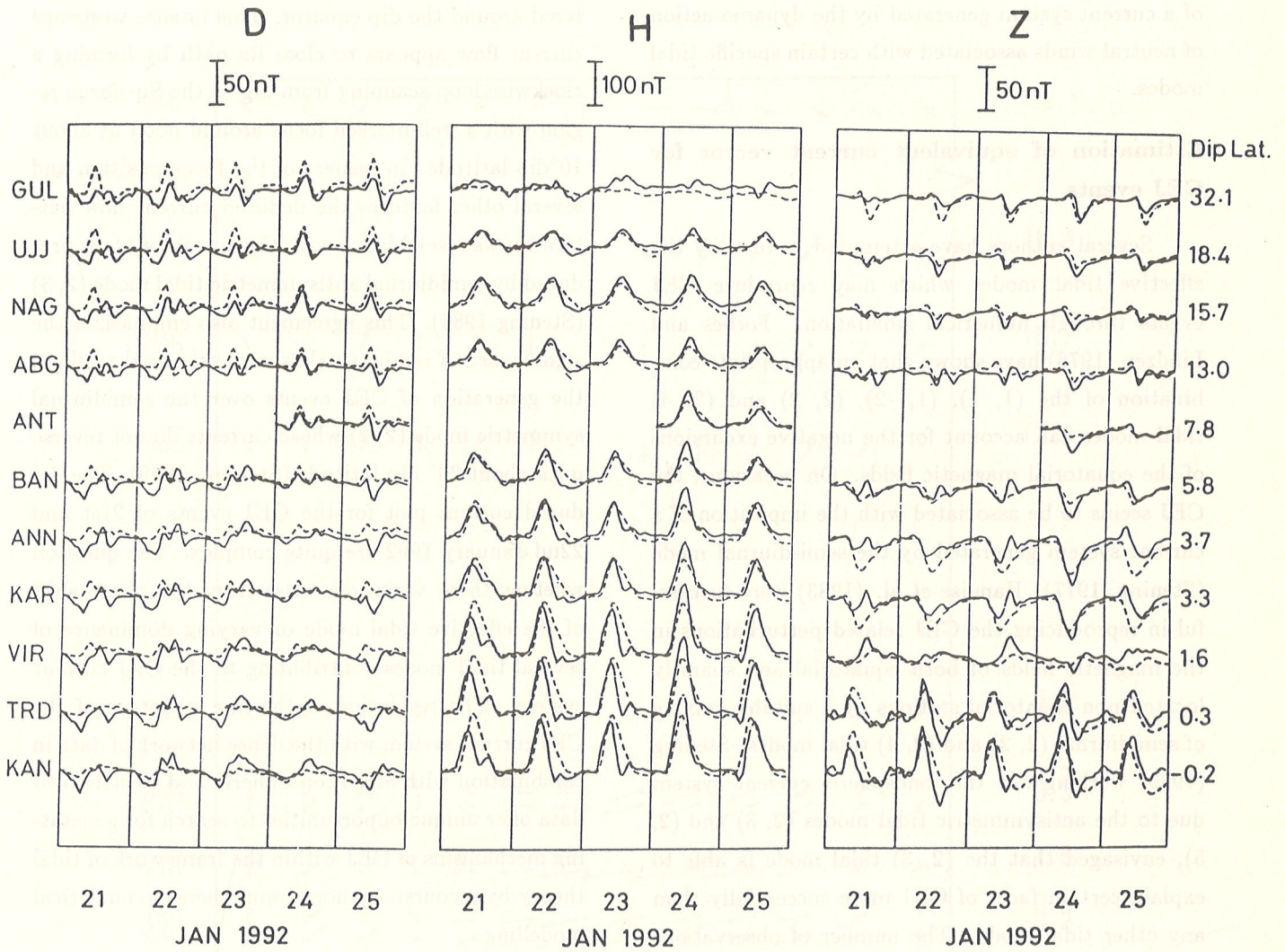
### Morphological Features

Fig. 7 gives the sequence of daily variation in D, H and Z (solid curves) recorded between 21st to 25th January, 1992. The broken curves in the figure represent the Sq variation based on five quiet-days of February, 1992 (adopted from Fig. 5). The  $A_P$  and 3-hr  $K_P$  values given in Table 2, indicate that all these days are relatively quiet. The daily variation in H, S(H), at the equatorial station exhibit negative depression in the afternoon hours (14-15 LT) on 21st, 22nd and 23rd January, 1992, while the S(H) on 25th January, 1992 is characterized by a negative excursion in the morning hours, around 08-09 LT. The variation on 24th January, 1992, depict a relatively strong Sq-pattern at all latitudes. Latitudinal profiles of S(H) and S(Z) corresponding to hours of maximum negative excursion are reversed in relation to the profile of Sq(H) and Sq(Z) at respective timings and form unambiguous evidence (Mayaud, 1977) for the existence of afternoon counter electrojet on 21st, 22nd and 23rd January, 1992, and morning counter

electrojet on 25th January, 1992. The examination of CEJ related daily variations, S(H) on CEJ days minus monthly mean Sq(H), reveals that a slow and smooth depression in  $\Delta H$  in the afternoon is preceded by a pronounced peak in the forenoon. This characteristics, first demonstrated by Bhargava and Sastri (1977), was used by Rastogi (1981) to classify such CEJ events to be manifestations of the luni-solar tidal effects. The comparison of S(H) and Sq(H) during intervals of the CEJ occurrence suggests that except in the event of 22nd January, 1992, the latitudinal extent of the CEJ related perturbation does not exceed the normally accepted width of the electrojet. Further, within the limits of stations spacing, latitudinal width of both morning and afternoon electrojet appears to be the same, though based on the data from central Africa it was deduced by Mayaud (1977) that the width of the morning counter-electrojet is little wider than that of the electrojet.

On the 22nd January 1992 CEJ event, scanning all afternoon hours, depression persists over the entire latitude range examined. Rastogi (1991) has given several more examples of the CEJ event where their effects were seen to extend from the dip equator to the region of Sq focus. The magnitude of depression in such events (as seen on January 22) decreases with increasing latitude and may perhaps represent CEJ events overriding some magnetic disturbance associated with ring current or substorm activity. The comparison with records from different longitudes may help identify the source.

The S(D) and S(Z) plots also show significant deviation from normal Sq-patterns within the equatorial belt. The perturbation in Z are most significant in the time-interval when CEJ related effects are pronounced in S(H). The sign of these deviations are consistent with what would result from the reversal of electrojet current centered around the dip equator. In D, the most significant changes are seen at low and middle latitudes (13-32° dip lat.). The presence



**Figure 7.** Sequence of daily-field variations in D, H and Z (solid lines) recorded during January 21-25, 1992 at stations functional during the first intensive observational campaign of the IEEY. Dashed curves represent normal  $S_q$  variation.

*Seqüência de variações diárias dos campos de D, H, e Z (linhas sólidas) registradas em janeiro 21 a 25, 1992, durante a primeira campanha intensiva de observações do AIEE. Linhas tracejadas representam as variações normais  $S_q$ .*

of significant perturbations away from the equatorial belt corroborate the hypothesis that the CFJ related effect may be viewed as some large-scale deformation of the normal dynamo currents due to the imposition of a current system generated by the dynamo action of neutral winds associated with certain specific tidal modes.

#### Estimation of equivalent current vector for CEJ events

Several authors have attempted to identify the effective tidal modes which may reproduce CEJ events through numerical simulation. Forbes and Lindzen (1976) have shown that an appropriate combination of the (1, 1), (1, -2), (2, 2) and (2, 4) tidal modes can account for the negative excursions of the equatorial magnetic fields. On occasions, the CEJ seems to be associated with the imposition of a current system generated by the semi-diurnal mode (Stening, 1977). Hanuise et al. (1983) were successful in reproducing the CEJ related perturbations in the magnetic fields of both equatorial and sparsely located non-equatorial stations by a suitable mixing of semidiurnal (2, 2) and (2, 4) tidal modes. Stening (1989) working out the ionospheric current system due to the antisymmetric tidal modes (2, 3) and (2, 5), envisaged that the (2, 3) tidal mode is able to explain certain facet of CEJ more successfully than any other tidal mode. The number of observations and their alignment permit better resolution of CEJ related current system than has been possible previously and may, thus, facilitate observational testing of the efficacy of the (2, 3) tidal mode in the production of the CEJ event.

To trace the dominant feature of the current system associated with the CEJ effect, the hourly inequalities in H and D, obtained by subtracting the normal Sq variation from CEJ days, were combined and the resulting magnetic vector rotated clockwise to yield an equivalent current vector. The deduced

current flow vectors associated with the CEJ event of Jan. 23, 1992 is given in Fig. 8 on a latitude-local time cross-section. The current flow pattern is dominated by a strip of westward directed current centered around the dip equator. This intense westward current flow appears to close its path by forming a clockwise loop scanning from dip to the Sq-focus region with a well marked focus around noon at about 10° dip latitude. In respect of the focus position and several other features the deduced current flow pattern shows resemblance with the current system produced by semidiurnal antisymmetric tidal mode (2, 3) (Stening 1989). This agreement also emphasizes the significance of semidiurnal asymmetric tidal mode in the generation of CEJ events over the semidiurnal symmetric mode (2, 2) whose currents do not reverse until about 20° dip latitude (Stening, 1989). The deduced current plot for the CEJ events of 21st and 22nd January 1992 are quite complex. The question whether these variations arise from the phase shift of the effective tidal mode or varying dominance of several tidal modes contributing to the CEJ current system. The resolution of the fine structure of the CEJ current system with the dense network of data in combination with allied ionospheric and electric field data offer unique opportunities to search for generating mechanisms of CEJ within the framework of tidal theory by recourse to more comprehensive numerical modelling.

#### GENERAL CONCLUSION AND FUTURE COURSE OF ACTION

The preliminary examination of the initial data set generated from the network of geomagnetic observatories along the Indian sector, especially upgraded for the IEEY period, reveal the following important features:

- (a) active intermixing of the Sq-vortices in the equatorial belt.
- (b) presence of strong induction effect, which dom-



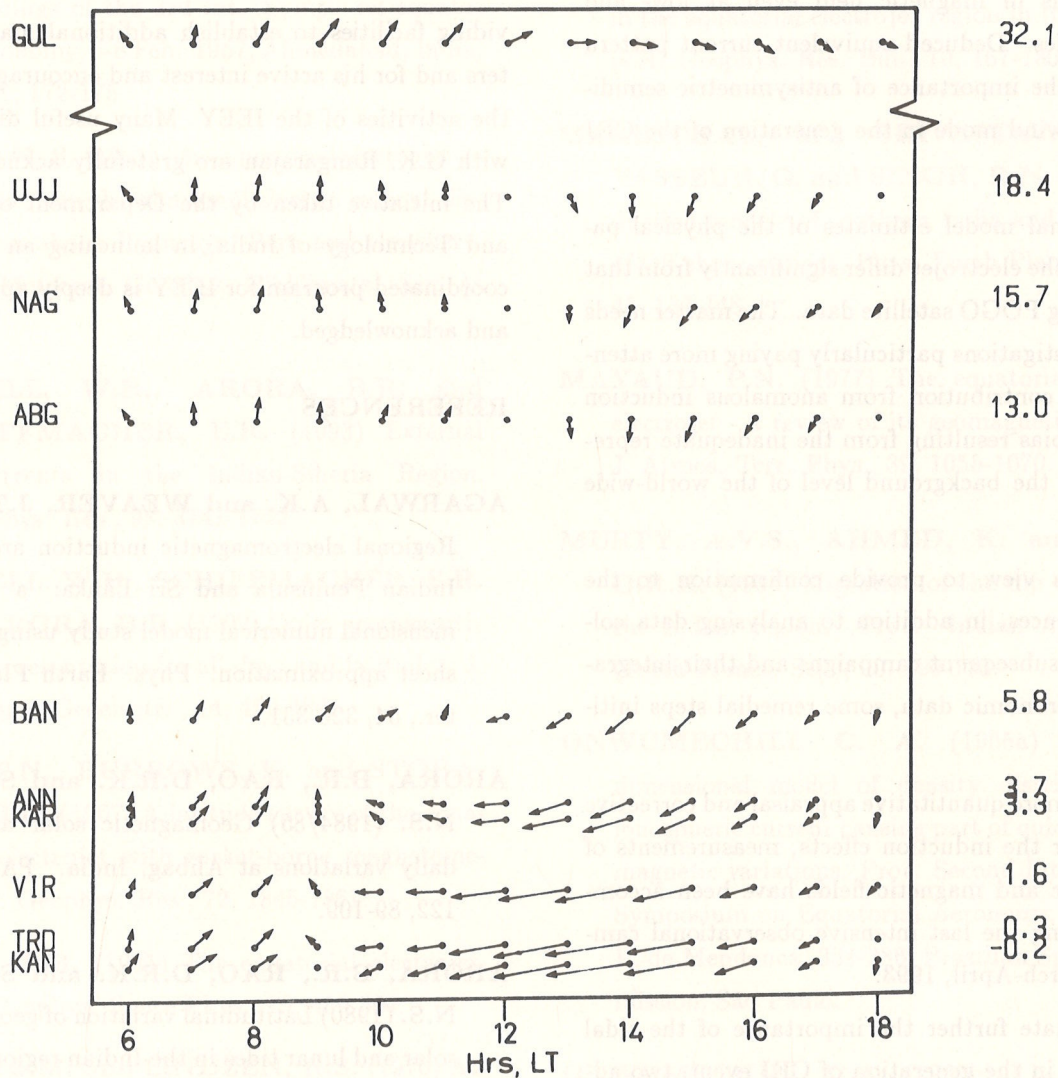


**Figure 8.** Pattern of total equivalent current (in arbitrary unit) associated with the counter electrojet event of January 23, 1992, determined by combining the hourly inequalities in D and H after subtracting the normal Sq variations.

*Esquema de corrente equivalente total (em unidades arbitrarias) associadas ao evento de eletrojoato reverso de 23 de janeiro de 1992, calculada combinando as desigualdades horarias em D e H após subtração das variações Sq normais.*

inate the diurnal and latitudinal characteristics of  $Sq(Z)$ .

(c) the EEJ (eastward) and CEJ (westward) current systems appears to have same latitudinal extent.

(d) evidence of strong and significant CEJ related perturbations in magnetic field even at low- and mid- latitudes. Deduced equivalent current pattern brings out the importance of antisymmetric semidiurnal tidal wind mode in the generation of the CEJ event.

(e) provisional model estimates of the physical parameters of the electrojet differ significantly from that derived using POGO satellite data. The matter needs further investigations particularly paying more attention to the contribution from anomalous induction effects and bias resulting from the inadequate representation of the background level of the world-wide  $Sq$ .

With a view to provide confirmation to the above inferences, in addition to analysing data collected from subsequent campaigns and their integration with aeronomic data, some remedial steps initiated are:

(i) towards more quantitative appraisal and corrective measures for the induction effects, measurements of both electric and magnetic fields have been accomplished during the last intensive observational campaign of March-April, 1993.

(ii) to evaluate further the importance of the tidal mode (2, 3) in the generation of CEJ event, two additional magnetometers are being operated in the latitude range of  $8^\circ - 12^\circ$  where the focus of the current vortex associated with this tidal mode is expected to prevail (Stenning, 1989).

(iii) to have a more precise estimate of  $Sq$  in the equatorial belt, the application of a "Slice-mirror" technique of spherical harmonic analysis, recently modified by Campbell et al. (1992, 1993) to obtain fine resolution  $Sq$  current system from a string of obser-

vatories in a single hemisphere, is envisioned by integrating present data with a Central Asia chain of observatories.

#### ACKNOWLEDGEMENTS

The authors thank the Director of IIG for providing facilities to establish additional magnetometers and for his active interest and encouragement in the activities of the IEEY. Many useful discussions with G.K. Rangarajan are gratefully acknowledged. The initiative taken by the Department of Science and Technology of India, in launching an all India coordinated program for IEEY is deeply appreciated and acknowledged.

#### REFERENCES

- AGARWAL, A.K. and WEAVER, J.T. (1989) Regional electromagnetic induction around the Indian Peninsula and Sri Lanka: a three dimensional numerical model study using the thin sheet approximation. *Phys. Earth Planet. Inter.*, 54, 320-331.
- ARORA, B.R., RAO, D.R.K. and SASTRI, N.S. (1984/85) Geomagnetic solar and lunar daily variations at Alibag, India. *PAGEOPH*, 122, 89-109.
- ARORA, B.R., RAO, D.R.K. and SASTRI, N.S. (1980) Latitudinal variation of geomagnetic solar and lunar tides in the Indian region. *Indian Acad. Sci. (Earth Planet. Sci.)*, 89, 333-346.
- ARORA, B.R. and SOMAYAJULU, V.V. (1991) Working document of the Indian contribution to the International Equatorial Electrojet Year. Unpublished Report of IIG, 1-37.
- BARTELS, J. and JOHNSTON, H.P. (1940) Geomagnetic tides in horizontal intensity at Huancayo. *Geophys. Res.*, 45, 269-308 and 485-592.

- BHARGAVA, B.N. and SASTRI, N.S.** (1977) A comparison of days with and without occurrence of counter electrojet afternoon events in the Indian region. *Ann. Geophys.*, 33, 329-333.
- CAIN, J.O.** (1969) The location of the dip equator, *Proceedings of the 3rd Int. Symp. on equatorial aeronomy*, 3-8 Feb. 1967, Ahmedabad, India, Vol. 1A, 172-175.
- CHAPMAN, S.** (1951) The equatorial electrojet as detected from the abnormal electric current distribution about Hyancayo, Peru and elsewhere. *Arch. Meteorol. Geophys. Bioklimatal*, Ser. A, 4, 368.
- CAMPBELL, W.H., ARORA, B.R. and SCHIFFMACHER, E.R.** (1993) External Sq currents in the Indian-Siheria Region. *J. Geophys. Res.*, 98, 3741-3752.
- CAMPBELL, W.H., SCHIFFMACHER, E.R. and ARORA, B.R.** (1992) Quiet geomagnetic field representation for all days and latitudes. *J. Geomagn. Geoelectri.*, 44, 459-480.
- DAVIS, T.N., BURROWS, K. and STORALIK, J.D.** (1967) A latitude survey of the equatorial electrojet with rocket-borne magnetometers. *J. Geophys. Res.*, 72, 1845-1861.
- FORBES, J.M.** (1981) The equatorial electrojet. *Rev. Geophys. Space Phys.*, 19, 469-504.
- FORBES, J.M. and LINDZEN, R.S.** (1976) Atmospheric solar tides and their electrodynamic effects, II. The equatorial electrojet, *J. Atmos. Terr. Phys.*, 38, 911-920.
- FORBUSH, S.E., CASAVARDE, M. and SCHMUCKER, V.** (1967) Annual Rep. for 1965-66, Dept. of Terr. Mag. Carnegie Inst. Wash.
- HANUISE, C., MAZAUDIER, C., VILA, P., BLANC, M. and CROCHET, M.** (1983) Global dynamo simulation of ionospheric currents and their connection with the equatorial electrojet and counter electrojet: A case study. *J. Geophys. Res.*, 88, 253-270.
- IIG, NGRI, SOI** (1972) Ground magnetic survey in the equatorial electrojet region in India: a report. *Geophys. Res. Bull.* 10, 167-180.
- MARESCHAL, M., SRIVASTAVA, B.J., VASSEUR, G. and SINGH, R.N.** (1987) Induction models of southern India and the effect of Off-shore geology, *Phys. Earth Planet. Inter.*, 45, 137-148.
- MAYAUD, P.N.** (1977) The equatorial counter electrojet - a review of its geomagnetic aspects. *J. Atmos. Terr. Phys.*, 39, 1055-1070.
- MURTY, A.V.S., AHMED, K. and RAO, D.R.K.** (1984) Migration of the dip equator in the Indian region. *Proc. Indian Acad. Sci. (Farth Planet. Sci.)*, 93, 129-133.
- ONWUMECHILI, C. A.** (1965a) A three-dimensional model of density distribution of ionospheric current causing part of quiet day geomagnetic variations. *Proc. Second International Symposium on Equatorial Aeronomy*, edited by F. de Mendonca, 384-386, Brazilian Space Commission, São Paulo.
- ONWUMECHILI, C.A.** (1965b) The magnetic field of a current model for part of geomagnetic Sq variation. *Proc. Second International Symposium on Equatorial Aeronomy*, edited by F. de Mendonca, 387-390, Brazilian Space Commission, São Paulo.
- ONWUMECHILI, C.A.** (1967) Geomagnetic variations in the equatorial zone, In: *Phys. Geomag. Phenomena (Book)*. Eds. Matsushita S. and Campbell, W.H., Chap. III-2, 425-507.

- ONWUMECHILI, C.A.** (1992) Study of the return current of the equatorial electrojet. *J. Geomagn. Geoelectr.*, 44, 1-42.
- ONWUMECHILI, C.A. and AGU, C.E.** (1981a) Longitudinal variation of equatorial electrojet parameters derived from POGO satellite observations. *Planet. Space Sci.*, 29, 627-634.
- ONWUMECHILI, C.A. and AGU, C.E.** (1981b) The relationship between the current and the width of the equatorial electrojet. *J. Atmos. Terr. Phys.*, 43, 573-578.
- ONWUMECHILI, C.A., AGU, C.E. and OZOEMENA, P.C.** (1989a) Effect of equatorial electrojet intensity on its landmark distances. *J. Geomagn. Geoelectr.*, 41, 461-467.
- ONWUMECHILI, C.A., OZOEMENA, P.C. and AGU, C.E.** (1989b) Landmark values of equatorial electrojet current and magnetic field along a meridian near noon. *J. Geomagn. Geoelectr.*, 44, 443-459.
- ONWUMECHILI, C.A. and OZOEMENA, P.C.** (1985) Latitudinal extent of the equatorial electrojet. *J. Geomagn. Geoelectr.*, 37, 193-204.
- OZOEMENA, P.C. and ONWUMECHILI, C.A.** (1987) Global variations of the POGO electrojet parameters during the solstices. *J. Geomagn. Geoelectr.*, 39, 625-636.
- RAJARAM, M., SINGH, B. P., NITYANANDA, N. and AGRAWAL, A. K.** (1976) Effect of the presence of a conducting channel between India and Sri Lanka on the features of the equatorial electrojet. *Geophys. J.R. astro. Soc.*, 59, 127-138.
- RANGARAJAN, G.K. and DEKA, R.C.** (1991) The dip equator over peninsular India and its secular variations. *Proc. Indian Acad. Sci., (Earth Planet. Sci.)*, 100, 361-368.
- RASTOGI, R.G.** (1981) Equatorial counter electrojet and interplanetary magnetic field, *Ind. J. Space Phys.*, 10, 1-15.
- RASTOGI, R.G.** (1991) Latitudinal extent of the equatorial electrojet effects in the Indian zone. *Ann. Geophysicae*, 9, 777-783.
- REDDY, C.A.** (1989) The equatorial electrojet. *PAGEOPH*, 133, 481-508.
- SAMPATH, S. and SASTRY, T.S.G.** (1979) Results from in-situ measurements of ionospheric currents in the equatorial region. *J. Geomagn. Geoelectr.*, 31, 373-397.
- SRIVASTAVA, B.J.** (1992) New results on the dip equator and the equatorial electrojet in India. *J. Atmos. Terr. Phys.*, 54, 871-880.
- STENING, R.J.** (1977) Magnetic variations at other latitudes during reverse equatorial electrojet. *J. Atmos. Terr. Phys.*, 39, 1071-1077.
- STENING, R.J.** (1989) A calculation of ionospheric currents due to semidiurnal antisymmetric tides. *J. Geophys. Res.*, 94, 1525-1531.
- THAKUR, N.K., MAHASHABDE, M.V., ARORA, B.R., SINGH, B.P., SRIVASTAVA, B.J. and PRASAD, S.N.** (1986) Geomagnetic variations anomalies in peninsular India. *Geophys. J.R. astr. Soc.*, 86, 839-854.
- YACOB, A.** (1967) The Indian equatorial electrojet in IGY and IGSY. *Indian J. Met. Geophys.*, 18, 285-288.
- YACOB, A. and KHANNA, K.** (1963) Geomagnetic Sq variations and parameters of the Indian electrojet for 1958 and 1959. *Ind. J. Met. Geophys.*, 14, 470-477.

Submetido em 18.06.93

Revisado em 10.12.93

Aceito em 11.01.94

Editor responsável V.W.J.H. Kirchhoff

# LONG TERM CHANGES IN THE SPORADIC E-LAYER PHENOMENA OVER PORTALEZA, BRAZIL

## Key words

IEEY

International Equatorial Electrojet Year

Ionosphere

Electrojet

Counter Electrojet

## Palavras chave

AIEE

Ano Internacional do Eletrojato Equatorial

Ionosfera

Eletrojato

Eletrojato Reverso